ChemEngineering

MDPI

Article

Combustion Air Humidifier for a Biomass Boiler with Flue Gas Condensation

Jan Havlík * and Tomáš Dlouhý

Department of Energy Engineering, Faculty of Mechanical Engineering, Czech Technical University in Prague, Technicka 4, 16600 Prague, Czech Republic; tomas.dlouhy@fs.cvut.cz

* Correspondence: jan.havlik@fs.cvut.cz

Abstract

This paper deals with combustion air humidification for application with a biomass boiler and a spray flue gas condenser. The use of a combustion air humidifier increases the dew point temperature of the flue gas, thereby increasing the potential for heat recovery in the flue gas condenser and increasing the amount of heat supplied to the thermal system. The air humidification process in a counter current spray humidifier was experimentally analysed under conditions corresponding to the use before a biomass boiler with a flue gas condenser. For air heating and humidification, temperature factor values of up to 0.90 can be obtained; this value is mainly influenced by the ratio of the spray water and humidified air flow rates. The volumetric heat transfer coefficient is significantly affected by the humidified air velocity, although this velocity is negligible compared to the counter current spray water velocity. The volumetric heat transfer coefficient reaches higher values at higher spray water temperatures and therefore higher air heating. The whole process is also affected by the saturation of the incoming air, where the dew point temperature of the air drawn in from the surroundings is lower than its temperature. These results can be used as basic information for the design of combustion air humidifiers, for the selection of their operating parameters, and for a basic balancing of the energy contribution of the combustion air humidifier before a more detailed design of the whole system.

Keywords: air humidifier; spray; biomass boiler; combustion air; heating; humidification

check for updates

Academic Editor: Dmitry Yu. Murzin

Received: 30 April 2025
Revised: 13 June 2025
Accepted: 23 June 2025
Published: 25 June 2025

Citation: Havlík, J.; Dlouhý, T. Combustion Air Humidifier for a Biomass Boiler with Flue Gas Condensation. *ChemEngineering* **2025**, *9*, 68. https://doi.org/10.3390/chemengineering9040068

Copyright: © 2025 by the authors. Licensee MDPI, Basel, Switzerland. This article is an open access article distributed under the terms and conditions of the Creative Commons Attribution (CC BY) license (https://creativecommons.org/licenses/by/4.0/).

1. Introduction

Nowadays, one of the main objectives in the design of energy sources for heat production is to maximise the overall efficiency and thus reduce fuel consumption. The use of flue gas condensers with biomass boilers is thus increasingly used in practice. The heat obtained from flue gas condensation can be used to preheat the return water from the district heating (DH) system [1,2]. If the difference between the dew point temperature of the flue gas and the temperature of the return water from the DH system is small, the heat obtained by flue gas condensation is minimal. The option is to install a combustion air humidifier, which increases the humidity of the flue gas and also its dew point temperature [1,3], thereby increasing the potential for heat recovery in the flue gas condenser. The use of a combustion air humidifier in a hot water biomass boiler system with a flue gas condenser can significantly increase the amount of heat supplied to the DH system, in the order of percent points of the boiler output, depending on the temperature of the heated air in the humidifier. For wood chips with 35 and 45% water content, the contribution to the heat input to the CHP system would be 7–9% of the boiler thermal output [3].

As combustion air humidifiers, it is suitable to use mixing spray heat exchangers in a vertical configuration, where combustion air sucked in from the surroundings is fed into the lower part. In the upper part there is a system of nozzles for spraying water (warm condensate from the flue gas condenser) into the cold air stream, which is thus heated and at the same time humidified by evaporated water vapour from the cooled condensate [1,2]. To increase the water–air contact surface, a packed bed can be placed under the nozzles [4,5]. The heated and humidified air is exhausted at the top, a demister is placed at the outlet of the heat exchanger to catch drifting droplets, and another heat exchanger is used to reheat the air above its dew point temperature to prevent condensation of moisture in the air ducts [1,2].

The advantage of using a packed bed in a spray heat exchanger is the high heat output relative to the volume of the device [4,5]. The disadvantages are the higher pressure drop, the occurrence of thermal gradients in the packed bed and the associated inhomogeneity of the process throughout the volume, and the difficulty of cleaning packed beds in case of clogging, e.g., if they contain small impurities in the used flue gas condensate [4]. The spray water must be distributed over the entire cross-section of the heat exchanger; therefore, part of the exchanger must always have a free cross-section and only after a certain distribution distance can the packed bed be used [6].

Standard air humidifiers are most often designed for air conditioning applications. Here, humidification with steam or water is used [7]. In this case, however, cold water is sprayed into a stream of warm air, which cools and transfers heat to the sprayed water, which then evaporates. The mechanism of the heat sharing process is thus different from the combustion air humidifier.

In the computational models of heat transfer between water droplets sprayed into the flowing air, the relative velocity between the sprayed droplets and the flowing air is used as the computational velocity to determine the Reynolds number needed to express the heat transfer coefficient [4,8]. Since the velocity of the sprayed droplets is significantly higher, the velocity of the flowing air can be neglected in the calculation [4,9]. However, according to the results of experiments carried out on the spray humidifier presented in [10], the value of the heat transfer coefficient (HTC) is dependent on the velocity of the flowing air. Thus, when water vapour evaporates from the surface of the droplets into the flowing air, where mass transfer occurs in the air, which gradually saturates with water vapour in the direction from the surface of the droplets to the main air stream, the mass transfer intensity can be expected to be influenced by the air velocity [11]. The question is whether heat transfer or mass transfer has a controlling influence on the entire process of humidifying and heating the air. In analytically derived computational models of heat transfer, the heat balance of the process is based on the knowledge of the equilibrium temperature at the phase interface of the water vapour evaporation, but in real cases this temperature cannot be precisely determined and can only be estimated on the basis of empirical experience [4].

Under similar conditions, humidifiers are operated during seawater desalination in systems called humidification–dehumidification desalination cycles [6,8,10,12–14], where heated water is sprayed through a nozzle into a stream of cold and saturated air. Their design is most often solved based on the description of mass transfer and its analogous transfer to heat transfer [6,14–17]. Again, these are empirically developed models. However, this calculation procedure does not take into account the heating of the gas itself, which is part of the process, and which can be expected to have a significantly lower heat transfer intensity than evaporation, which can fundamentally affect the whole process. The ratio of the heat output for the evaporation of water vapour and simultaneous heating of air can vary with both the initial air temperature and the initial relative humidity.

For energy balancing of a hot water boiler system with flue gas condenser and evaluation of the benefits of combustion air humidifier application, it is necessary to estimate the level of heating and thus humidification of the air with respect to the temperature of the spray water before the design of the whole system [3]. This value can only be estimated at this stage of the design process. The dependence of the amount of moisture absorbed into the air during heating is not linear, as the temperature increases the amount of water vapour required to achieve air saturation increases significantly, increasing the potential heat output transferred and the energy effect of the whole system. Thus, the aim of the process is to heat the air to as high a temperature as possible, i.e., as close as possible to the temperature of the shower water, which also means a higher specific humidity achieved.

The benefits of using a combustion air humidifier in a boiler system with a flue gas condenser are described and quantified in the literature. However, the actual design of the humidifier for these applications is not described in detail in the literature. In general, although heat and mass transfers for humidification are also described for packed bed heat exchangers for commonly used humidifiers mainly for air conditioning applications, these operate on a different principle.

The aim of this paper is to analyse the combustion air humidification process for a biomass boiler application where a flue gas spray condenser is connected and to experimentally verify the potentially achievable heating and humidification of the air in the spray humidifier. An important output is the determination of the parameters affecting the operation of these devices, based on which recommendations for the design of combustion air humidifiers will be formulated. These outputs can be used as baseline information for the design of combustion air humidifiers, for the selection of operating parameters to optimise its operation with respect to achieving the highest possible heating and humidification of combustion air, and for a basic balancing of the energy benefits of the combustion air humidifier prior to a more detailed design of the overall system.

2. Materials and Methods

2.1. Combustion Air Humidifier

Air humidifiers are most often made up of a combination of two parts: the spray zone, where heat transfer takes place on the surface of the sprayed droplets, and the packed bed zone, where heat transfer takes place on the surface of the water film that flows over the bed [6,12]. Thus, the heat transfer mechanism in each of these regions differs significantly.

Heat transfer at the surface of a droplet that is enveloped by the flowing gas is a case described in detail in the literature. When describing the heat transfer for spray heat exchangers, the relative velocity between the spray water and the flowing gas is considered as the calculation velocity. The flow velocity of the spray droplets is usually significantly higher than the flow velocity of the humidified air, so the calculation velocity can only be considered as the droplet velocity. In a counter current arrangement, the relative velocity is

$$w_{dr-a} = w_{dr} + w_a \approx w_{dr}. \quad (1)$$

It follows that the gas velocity w_a should not affect the value of the HTC. In the calculation of the HTC, the gas flow velocity is not taken into account, although it can have a significant effect on the mass transfer in the gas, i.e., specifically on the diffusion of evaporated water vapour from the surface of the droplets into the gas stream and its uniform saturation [4].

Empirically derived equations can be used in the design of a packed bed heat exchanger [4]. Another possibility is to use the analogy between heat and mass transfers derived from the mass transfer during evaporation of water vapour into air for the calcu-

lation of heat transfer [15,18–20]. However, these calculation procedures do not take into account the heating of the gas itself, which is part of the process and can be expected to have a significantly lower intensity of heat transfer. The amount of water vapour absorbed when the air reaches a state of water vapour saturation does not have a linear dependence on its temperature (Figure 1). At higher air temperature, the same change in the specific humidity corresponds to a smaller change in air temperature. Therefore, as the temperature changes, the ratio of heat for heating the air and evaporating water vapour also changes.

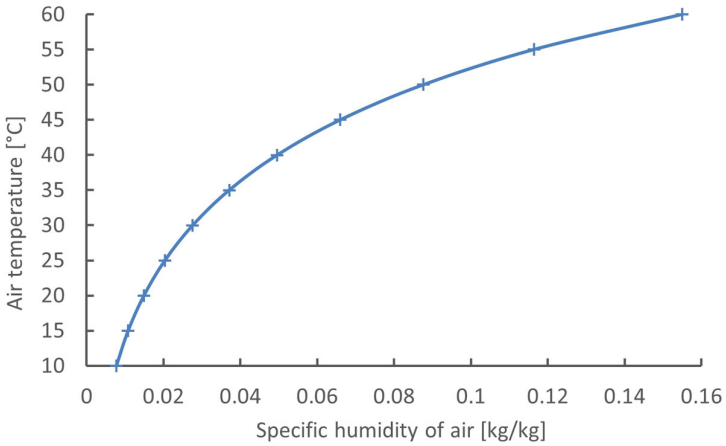

Figure 1. Dependence of air temperature on specific humidity.

2.2. Experimental Setup

The experimental combustion air humidifier (Figure 2) has a cylindrical shape with an inner shell diameter of 200 mm, is made of stainless steel, and its surface is thermally insulated to minimise temperature losses. The humidifier is composed of several rearrangeable modules. The lower module is used for the air inlet and spray water outlet of the humidifier. The 200 mm high module has a grid with square meshes at the bottom for the placement of the packed bed (made of Raschig rings). The diameter of the rings and the height of their layers can be freely changed. Another module with a height of 377 mm houses the shower water inlet and the spray nozzle. A last module has a demister to catch droplets that may be entrained by the heated air stream.

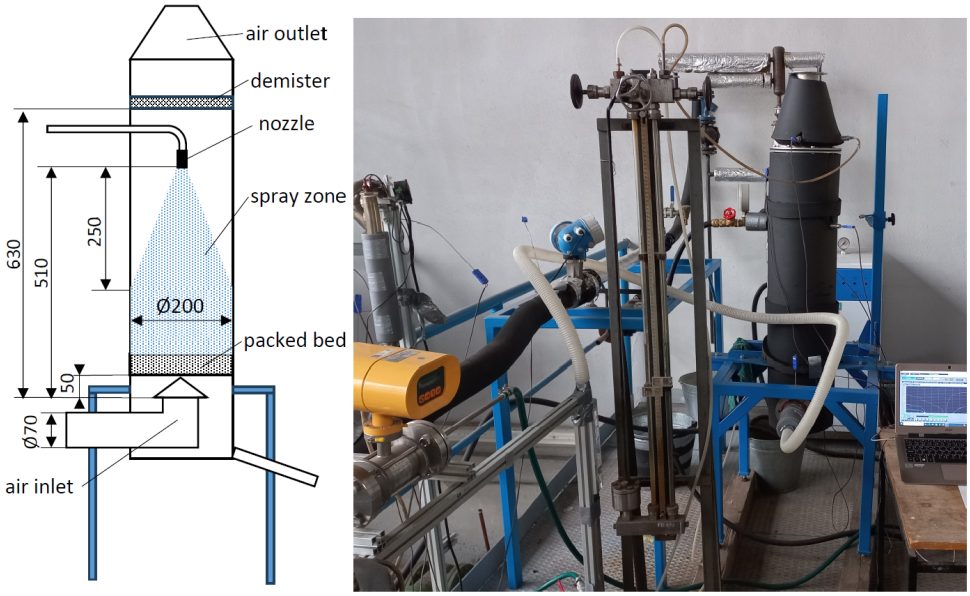

Figure 2. Air humidifier and its connection to experimental loop.

During the experiments, the humidifier is always operated in counter current operation. The spraying of the water is performed by a nozzle that provides an axial type of spray with a full cone. The use of this nozzle is appropriate as the water stream is evenly distributed in the form of droplets over the entire cross-section of the humidifier section. Nozzle 490.403.1Y.CA from Lechler (Metzingen, Germany) was used in the experiments. The nozzle is made of stainless austenitic steel 1.4404, the spray angle is 45° (more detailed technical data can be found in Appendix A, Figure A1). The size of the sprayed droplets was determined by using Spraytec equipment (Malvern Panalytical Ltd., Malvern, UK) to measure the droplet size distribution by laser light diffraction technique. The calculated droplet size is given as the average value of the Sauter diameter over the measured section as a function of the cooling water pressure at the nozzle inlet. The Sauter diameter is defined as the diameter of a droplet having the same value of the ratio of its volume to its surface area as the ratio of the volume of all droplets to their total surface area.

The flow rate and pressure of water in the spray nozzle were kept constant for all measurements. For these conditions, the experimentally determined droplet size was expressed using the Sauter diameter as 0.280 mm. The flow velocity of the spray droplets at the nozzle orifice is 13.2 m/s. Glass Raschig rings with a diameter of 10 mm and a specific surface area of 440 m^2/m^3 were used in the experiments.

A diagram of the experimental setup is shown in Figure 3. Air is supplied from a compressor with a large air tank to the lower part of the humidifier. Before entering, the air flow rate, pressure, temperature, and relative humidity are measured. In the upper part of the humidifier, there is a water drop separator for the case of drifting. Thermocouples are placed at the inlet and outlet in several places along the cross-section of the exchanger to measure air temperature. Pressure sensors are placed at the air inlet and outlet to determine the pressure loss of the humidifier. However, at such low air speeds, the loss is minimal and reaches maximum values up to 10 Pa. Water used for showering is heated in an electric boiler to the required temperature before entering the heat exchanger (HUM). The cooling water flow rate is measured by a FLONET FN2010.1 induction flowmeter (Elis Pilsen Ltd., Pilsen, Czech Republic) with current output calibrated with a deviation of 0.6%. Calibrated type-T thermocouples to within 0.2 °C are used to measure all temperatures. The air volume flow rate is measured by an IN-ECO PL3 rotameter (IN-ECO Ltd., Ružomberok, Slovakia) with accuracy of ±5%. The air pressure is measured by a U-tube water manometer and the relative humidity is measured with a Testo 400 hygrometer (Testo SE & Co. KGaA, Schwarzwald, Germany). The measured values are recorded at 5 s intervals in the DAS240Bat data logger.

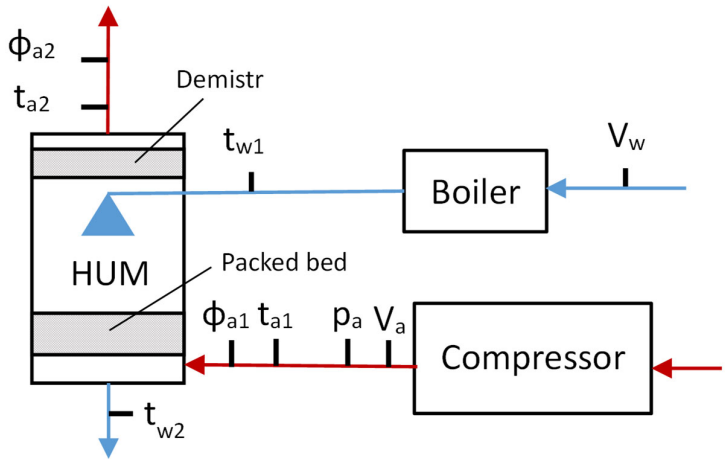

Figure 3. A diagram of the experimental setup with the main measured parameters indicated.

In the diagram, the letter t symbolises temperature measurement, the letter p symbolises pressure measurement, the letter V symbolises volume flow rate measurement, and the letter ϕ symbolises relative air humidity measurement. The index "w" indicates quantities related to the cooling water flow and the index "a" indicates quantities related to the air flow. The red colour indicates the air path and the blue colour indicates the spray water path.

2.3. Evaluation of Experiments

The evaluation of experimentally measured values includes balance calculations, both mass and energy. The heat transfer rate for heating and humidification of air Q_a is given by

$$Q_a = m_{da} \cdot (h_{da2} - h_{da1}) + m_{wv2} \cdot h_{wv2} - m_{wv1} \cdot h_{wv1}, \quad (2)$$

where h_{da} and h_{wv} are the enthalpies of dry air and water vapour for the corresponding temperatures. The mass flow rates of dry air m_{da} and water vapour contained in air m_{wv1} are determined from the measured volumetric flow rate $\dot{V}_a$.

$$\frac{m_{da}}{\rho_{da}} + \frac{m_{wv1}}{\rho_{wv}} = \dot{V}_a, \quad (3)$$

when

$$m_{wv1} = x_1 \cdot m_{da}, \quad (4)$$

where x is the specific humidity of the air expressed from its measured relative humidity as

$$x = 0.622 \frac{p_p}{p - p_p} = 0.622 \frac{\varphi \cdot p''_p}{p - \varphi \cdot p''_p}, \quad (5)$$

where p is the total air pressure and p''_p is the partial pressure of saturated water vapour for a given air temperature. By combining Equations (10) and (11) and modifying, then m_{da} can be calculated as

$$m_{da} = \frac{\dot{V}_a}{\frac{1}{\rho_{da}} + \frac{x_1}{\rho_{wv}}}. \quad (6)$$

The mass flow rate of water vapour contained in the outlet air can be determined as

$$m_{wv2} = x_2 \cdot m_{da}. \quad (7)$$

The amount of water evaporated from the spray water to the air $m_{\Delta W}$ is

$$m_{\Delta W} = m_{da} \cdot (x_{a2} - x_{a1}). \quad (8)$$

The heat transfer rate from the spray water Q_w can be calculated as follows:

$$Q_w = m_{w1} \cdot h_{w1} - \mathrm{m}_{w2} \cdot h_{w2}, \quad (9)$$

where $m_{w1,2}$ are the mass flow rates of cooling water at the inlet and outlet of the humidifier, and $h_{w1,2}$ are the enthalpies of cooling water for a corresponding temperature, where the difference in the mass flow rate of cooling water between the inlet and outlet of the humidifier corresponds to the amount of water evaporated.

$$m_{w2} = m_{w1} - m_{\Delta W}. \quad (10)$$

The overall balance of heat output is given as

$$Q_w = Q_a + Q_{loss}, \tag{11}$$

where Q_{loss} is the heat loss of the heat exchanger. The heat losses were analysed based on the heat flux balance calculation. Knowing the thickness of the thermal insulation (t_{in} = 25 mm), its thermal conductivity (λ_{in} = 0.04 W/mK), the temperature on the inside wall $T_{w,i}$, and the ambient temperature T_{amb}, the heat transfer rate from the insulation to the surroundings can be calculated for the estimated heat transfer coefficient between the insulation and the surroundings (α_{amb} = 10 W/m^{2}K). When the heat flux through the insulation and into the surroundings is equal

$$\frac{\lambda_{in}}{t_{in}} \cdot (T_{w,i} - T_{in,o}) = \alpha_{amb} \cdot (T_{in,o} - T_{amb}), \tag{12}$$

where $T_{in,o}$ is the temperature on the outer wall of the insulation. Assuming that the temperature drop in the steel wall of the heat exchanger is negligible, the temperature $T_{w,i}$ is determined as the value of the mean temperature of the humidified air. The temperature T_{amb} corresponds to the temperature at which the relative humidity of the inlet air is measured. $T_{in,o}$ can be expressed from Equation (12), and then Q_{loss} is calculated as

$$Q_{loss} = \alpha_{amb} \cdot A_{amb} \cdot (T_{in,o} - T_{amb}) \tag{13}$$

A_{amb} is the insulation surface between the measured temperature locations (A_{amb} = 0.677m^2). The individual heat loss values for each measurement are given in Appendix C, Table A2.

The heat transfer rate only for air heating $Q_{a-heating}$ is determined as

$$Q_{a-heating} = m_a \cdot c_{p,da} \cdot (t_{a2} - t_{a1}), \tag{14}$$

where $c_{p,da}$ is the specific heat capacity of dry air ($c_{p,da}$ = 1.01 kJ/kgK). The use of the volumetric HTC has the advantage of giving a better view of the overall size of the heat exchanger within the whole system, while simplifying the sizing of these devices. The volumetric HTC α_V is evaluated using the following relationship:

$$\alpha_V = \frac{Q_w}{V_{hum} \cdot \Delta T}, \tag{15}$$

where V_{hum} is the total volume of the heat exchange section determined as the volume of the cylinder whose diameter is the inner diameter of the humidifier, and the height is the vertical distance of the nozzle mouth from the inlet at the bottom of the section. The mean temperature difference ΔT can be determined for a humidifier as follows:

$$\Delta T = \frac{(T_{w1} + T_{w2}) - (T_{a1} + T_{a2})}{2}. \tag{16}$$

The molar flux n [kmol/m^{2}s] is determined from the amount of evaporated water relative to the droplet surface S_{dr} and the molar mass of water M_w.

$$n = \frac{m_{\Delta W}}{S_{dr} \cdot M_w} \tag{17}$$

When a packed bed is used, the surface area of the packed bed is calculated from its volume V_{pb} and specific surface a, and the total calculation area is then corrected by this surface.

$$S_{pb} = V_{pb} \cdot a \tag{18}$$

The mass transfer coefficient β is then expressed from the following equation:

$$n = \frac{\beta \cdot p}{R \cdot T} ln\left(\frac{1 - y_w}{1 - y_a}\right). \tag{19}$$

where R is the gas constant for air, T is the thermodynamic temperature, p is the total plaque, and y_w and y_a are the mole fractions at the surface of the interfacial interface and in the main gas stream determined from the ratio of the partial pressure of water vapour p_{sat} at the corresponding temperature and the total gas pressure.

$$y_w = \frac{p_{sat}(T_w)}{p};\ y_a = \frac{p_{sat}(T_a)}{p} \tag{20}$$

2.4. Uncertainty Analysis

The uncertainty analysis of the experimental results was carried out according to the procedure described in [21,22]. The uncertainties of the measured quantities are transferred to the quantities calculated according to the rules for the evaluation of the standard uncertainty by functional relations with uncorrelated variables [22]. The uncertainty of the experimental determination of the HTC is significantly different for measurements with shower water at 40 °C and 60 °C, which is due to the different achieved heat output and the level of the water cooling (its temperature difference). The uncertainty values for the volumetric HTC were in the range of 3 to 6% and 5 to 12% with a 95% confidence interval for water at 60 °C and 40 °C, respectively. Higher uncertainty values correspond to measurements with lower humidified air flow. The uncertainty for the mass transfer coefficient determined from the measurements is not as sensitive to changes in measurement conditions and was from 5 to 6% with a 95% confidence interval for all measurements. This is because its value is influenced by the primary inaccuracy of the air flow measurement.

3. Results and Discussion

The main parameters that affect the operation of a spray humidifier are the temperature of the spray water and the ratio of the flow rates of spray water and humidified air. Balance calculations for the integration of a combustion air humidifier into the system of a biomass boiler with a flue gas condenser connected to the DH system show that the temperature of the spray water should be around 60 °C and the ratio of the mass flow rates of spray water and humidified combustion air should be around 8:1 [3]. The operation of the experimental humidifier was verified in a wider range of operating parameters, but the aim was to measure the humidifier in a range close to the above parameters.

The experiments were performed with a base spray water temperature setting of approximately 60 °C. The mass flow ratios of the shower water and humidified air were set between 3:1 and 22:1. For these parameters, three configurations of the humidifier were analysed while maintaining a spray nozzle working height of 460 mm:

(1) Without packed bed (without).
(2) With packed bed of Raschig rings with a volume of 300 mL ≈ a layer of cca 1 cm (RR300).
(3) With packed bed of Raschig rings with a volume of 1400 mL ≈ a layer of cca 5 cm (RR1400).

In a comparative series of experiments, measurements were made with identical parameter settings, with the only difference being the inlet temperature of the spray water, which was set to approximately 40 °C to demonstrate the effect of temperature. An overview of the experimental data is presented in Appendix B, Table A1. The relative humidity at the humidifier outlet reached 100% in all measurements. The air therefore always leaves the heat exchanger saturated with moisture to the maximum possible level. For all measurements, the heat balance of the heat exchanger was checked by comparing the heat transfer rater on the water and air side; the results of the balances for all measurements are presented in Appendix C, Table A2. Figure 4 shows an example of the temperature distribution in the humidifier depending on the ratio of the mass flow rates of spray water and humidified air for configuration (1).

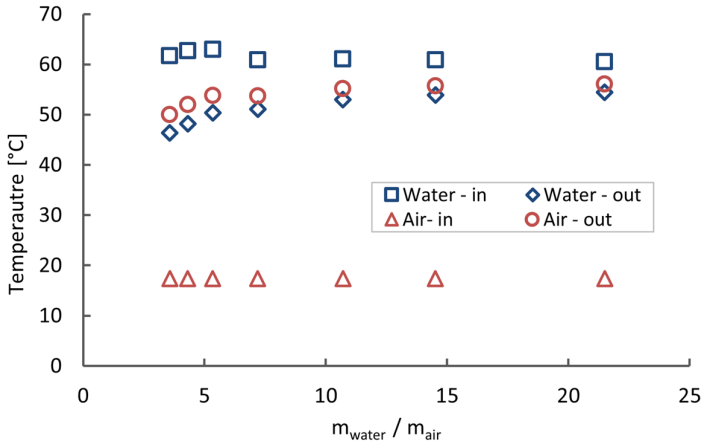

Figure 4. Inlet and outlet temperatures of humidified air and spray water for various ratio of their mass flow rates.

From the measured temperatures, the end temperature differences in the humidifier, i.e., the temperature differences at the inlet of the spray water and at the outlet of the heated air, were evaluated. The results show the influence of the flow rate ratio of both media on their outlet temperatures, which is in agreement with the experimental results presented in [15,20]. For a reference media mass flow rate ratio of 8:1 and the use of a packed bed, an end temperature difference of about 4 °C can be achieved. For a more general view and portability of the results, it is convenient to express the final temperature differences in relative values. In Figure 5, the relative end temperature differences are expressed as so-called temperature factors (ratio of the actual air heating to the maximum possible theoretical heating to the inlet spray water temperature). The heat exchanger temperature factor is given as the ratio of the real temperature difference for heating to the maximum possible temperature difference.

$$\frac{dT}{dT_{max}} = \frac{T_{a,out} - T_{a,in}}{T_{w,in} - T_{a,in}} \tag{21}$$

To the measurements already presented (spray water temperature of 60 °C), a comparison with the values measured for a spray water temperature of 40 °C is added. For the reference ratio of spray water and humidified air mass flow rates in real humidifier operation of 1:8 and a spray water temperature of 60 °C, a temperature factor value above 0.90 can be achieved.

The difference in the resulting values for the series labelled 60 °C and 40 °C is due to the fact that for higher values of the temperature factor (40 °C series), the heat exchanger heat output is lower. Therefore, for the same sized heat exchanger, it is possible to achieve a smaller

end temperature difference at the outlet of the humidifier (difference between outlet heated air temperature and inlet shower water temperature) and thus higher temperature factors.

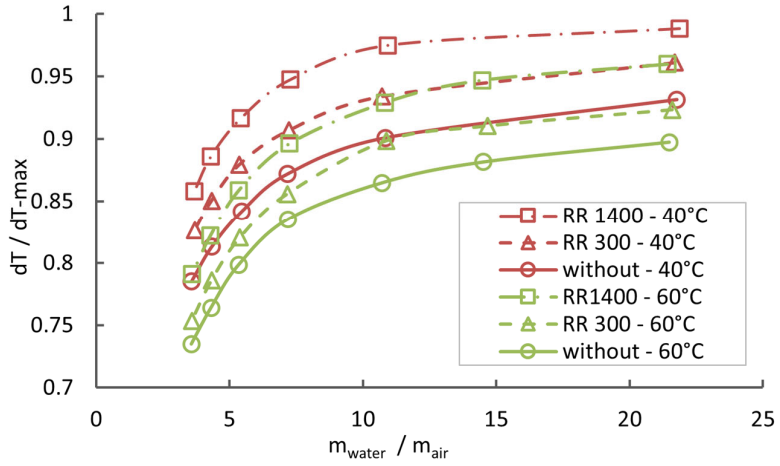

Figure 5. Relative end temperature difference as function of media flow rate ratio.

The experimentally determined values of the volumetric HTC as a function of the ratio of the mass flow rates for different water temperatures and different configurations are shown in Figure 6. According to the conclusions of [15], the temperature of the spray water is an essential process parameter. From Figure 6, it can be seen that higher values of the volumetric HTC are achieved at higher spray water temperatures and hence higher outlet air temperature.

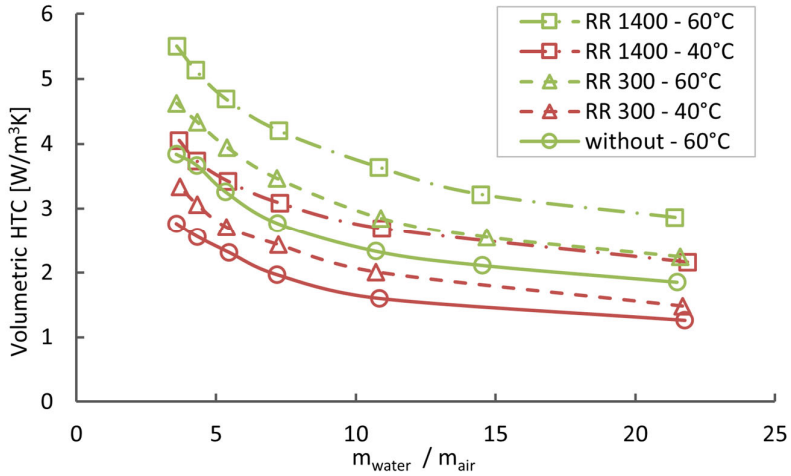

Figure 6. The dependence of the volumetric HTC on the ratio of the media flow rates.

The results of the experiments show that the volumetric HTC is significantly influenced by the velocity of the humidified air, although this velocity is negligible relative to the counterflow velocity of the spray water and the relative velocity of both media, which is standardly used in heat transfer calculations in spray heat exchangers.

This is probably since the determining process in humidification is the diffusion of evaporated water vapour on the surface of the spray water droplets into the flowing air. The intensity of the mass transfer in the transport of the droplets into the flowing air is dependent on the air velocity, with the process being more intense at higher air velocity values.

The relative difference between the experiments for spray water temperatures of 40 °C and 60 °C is shown in Figure 7. It can be seen that the ratio of the values of these

coefficients is very similar over the entire interval analysed (values in the ratio range 0.7 to 0.8). This indicates that the value of the volumetric HTC is significantly influenced by the temperature of the humidified air. At the same time, knowing the ratio of the values of the volumetric HTCs for two different temperatures at the same ratio of flow rates, it is thus possible to recalculate the value of the volumetric HTC from one temperature to the other temperature for any value of the flow rates.

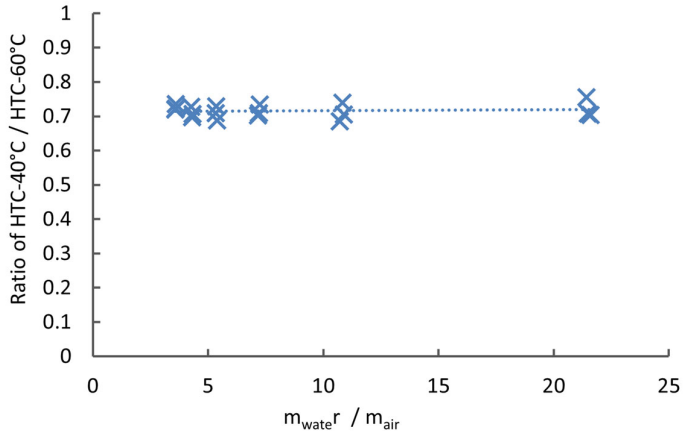

Figure 7. Ratio of volumetric HTC values for spray water temperatures of 40 °C and 60 °C.

An Analysis of the Effect of Spray Water Temperature and Air Velocity on Heat and Mass Transfer in the Humidifier

Figure 8 shows the dependence of the mass transfer coefficient of water vapour evaporation in the humidifier on the air flow velocity for different spray water temperatures and configurations. The values of the mass transfer coefficient increase with the packed bed layer size but, on the contrary, are not significantly affected by the humidified air temperature.

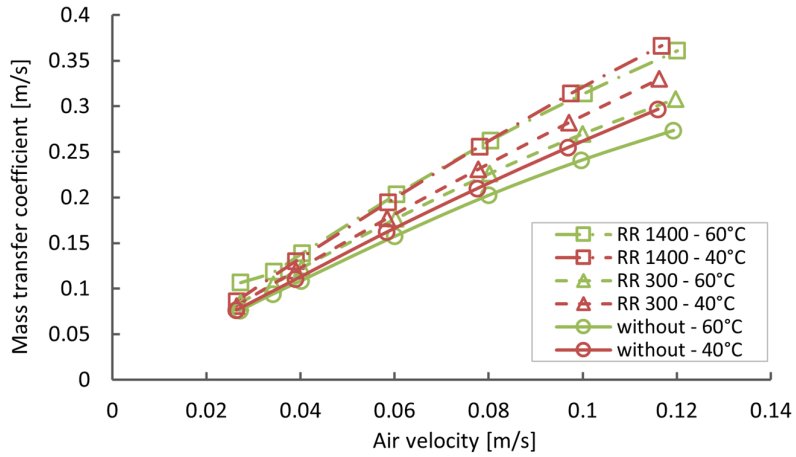

Figure 8. The dependence of mass transfer coefficient on the air velocity in the humidifier for different spray water temperatures.

In Figure 9, the dependence of the volumetric HTC on the air flow velocity is shown. The use of a packed bed significantly increases the volumetric HTC values and thus the heat output. So it is possible to achieve a smaller heat exchanger size for the same heat output.

In accordance with the experimental results obtained in [10], the HTC in a spray humidifier is significantly dependent on the air velocity. However, a comparison of the course in Figures 8 and 9 shows a discrepancy between the heat transfer and mass transfer dependencies, where the mass transfer values are not significantly affected by the gas temperature, while the heat transfer values are significantly affected by the gas temperature.

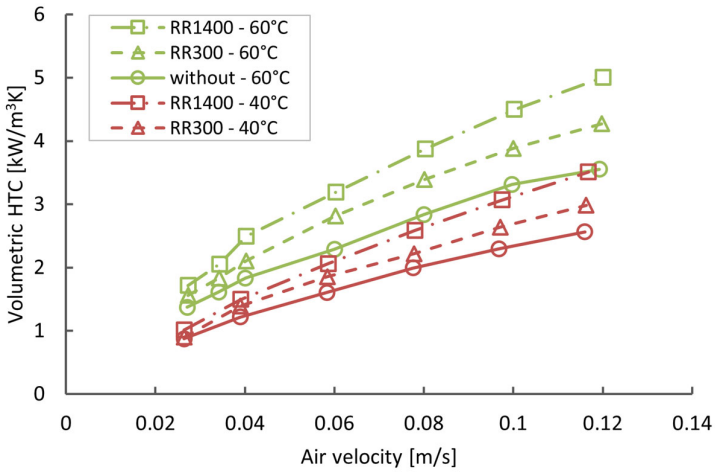

Figure 9. The dependence of the volumetric HTC on the air velocity in the humidifier for different spray water temperatures.

The values of the volumetric HTC are higher at higher spray water temperatures and therefore higher air temperatures. This agrees with the results presented in [10], where this phenomenon is explained by the change in relative humidity at higher temperatures and thus the change in water vapour concentration. However, this would simultaneously affect the mass transfer rate, which is not consistent with the results in Figure 8, where the mass transfer coefficient is not significantly dependent on temperature. Rather, the explanation may be that as the temperature of the outlet humidified air increases, the ratio of the heat required to heat the air to the heat required to humidify it (water vapour saturation) decreases. The ratio of the heat required to heat the air to the total heat required to heat and humidify the air from an initial temperature of 15 °C for initial relative humidities of 50% and 100% to the desired outlet saturated air temperature is shown in Figure 10. Thus, at higher temperatures, more of the heat is used for evaporation, which may result in an increase in the mean value of the volumetric HTC.

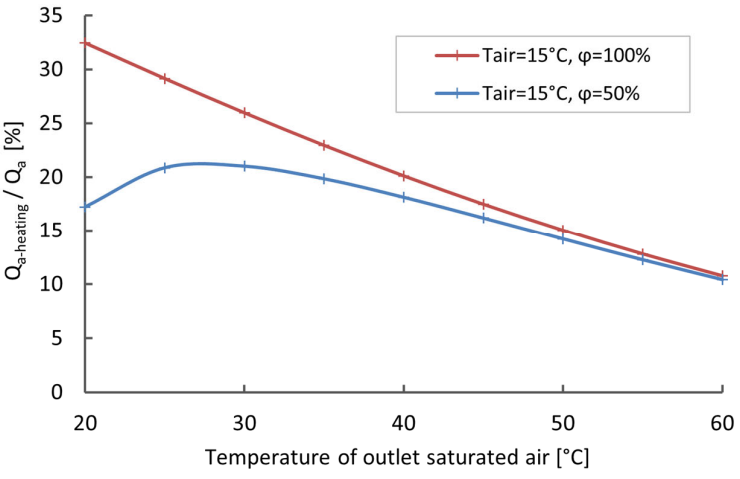

Figure 10. Proportion of heat used for air heating only out of total heat required for heating and humidification.

In accordance with the findings of [16], the whole process is also influenced by the saturation of the incoming air (its relative humidity), where the dew point temperature of the air drawn in from the surroundings is therefore lower than its temperature. Thus, in the initial phase of the process, only the saturation of the air with water vapour occurs without a change in its temperature, which will increase the amount of heat used for evaporation of

the water vapour and thus the total amount of heat. As a result, the ratio of heat used for heating to total heat used is reduced.

4. Conclusions

The air humidification process in a counter current spray humidifier was experimentally analysed. It was confirmed that when heating the air in conditions corresponding to the humidification of combustion air applied to a biomass boiler with a spray flue gas condenser, it is possible to achieve temperature factor values (the ratio of the difference between the outlet temperature of the humidified air and the inlet temperature to the difference between the inlet temperature of the spray water and the inlet temperature of the humidified air) above 0.90. This value is influenced by the ratio of the flow rates of the spray water and the humidified air.

The volumetric HTC is significantly influenced by the humidified air velocity, although this velocity is negligible relative to the counterflow velocity of the spray water and thus the relative velocity of both media, which is standardly used as a calculation parameter for heat transfer calculations in spray heat exchangers.

This is probably due to the fact that the determining process in humidification is the diffusion of evaporated water vapour from the surface of the spray water droplets into the flowing air. The intensity of mass transfer in the transport of droplets into the flowing air is dependent on the air velocity, with the process being more intense at higher air velocity values.

The values of the volumetric HTC are higher at higher spray water temperatures and therefore also higher air heating. This may be since, as the temperature of the outlet humidified air increases, the ratio of the heat required to heat the air to the heat required to humidify the air (water vapour saturation) decreases. The heat transfer intensity of the phase change is significantly higher than that of the heating. Thus, at higher temperatures, more of the heat is used for evaporation, which can result in an increase in the mean value of the HTC.

The whole process is also affected by the saturation of the inlet air, where the dew point temperature of the air drawn in from the surroundings is lower than its temperature. Thus, at the initial stage of the process, only the air is saturated with water vapour without any change in temperature.

Author Contributions: Conceptualization, J.H. and T.D.; methodology, J.H. and T.D.; formal analysis, J.H.; investigation, J.H.; data curation, J.H.; writing—original draft preparation, J.H.; writing—review and editing, T.D.; visualisation, J.H.; supervision, T.D.; funding acquisition, T.D. All authors have read and agreed to the published version of the manuscript.

Funding: This research was funded by the Technology Agency of the Czech Republic, project no TK04030297.

Data Availability Statement: The original contributions presented in this study are included in the article. Further inquiries can be directed to the corresponding author.

Conflicts of Interest: The authors declare no conflicts of interest.

Nomenclature

a	specific surface, m^2/m^3
cp	specific heat capacity, J/kgK
D	diffusion coefficient, m^2/s
DH	district heating
d	diameter, m
h	specific enthalpy, kJ/kg
HTC	heat transfer coefficient

Lef	Lewis factor
m	mass flow rate, kg/s
Nu	Nusselt number
p	pressure, Pa
Pr	Prandtl number
n	molar flux, kmol/m^{2}s
Q	heat transfer rate, W
Re	Reynolds number
RR	Raschig rings
S	surface, m^2
St	Stanton number
St_m	mass Stanton number
t	temperature, °C
x	specific humidity, kg/kg
V	volume, m^3
$\dot{V}$	volume flow rate, m^3/s
y	molar fraction, mol.%
w	velocity, m/s
α	heat transfer coefficient, W/m^{2}K
α_V	volumetric heat transfer coefficient, kW/m^{3}K
β	mass transfer coefficient, m/s
ϕ	relative humidity,%
λ	thermal conductivity, W/mK
μ	dynamic viscosity, Pas
ν	kinematic viscosity, m^2/s
ρ	density, kg/m^3
ΔT	temperature difference, °C
Subscripts	
a	air
amb	ambient
dr	droplet
da	dry air
G	gas
L	liquid
o	outer
pb	packed bed
sat	saturated
w	water
wv	water vapour
ΔW	evaporated water
1	inlet
2	outlet

Appendix A

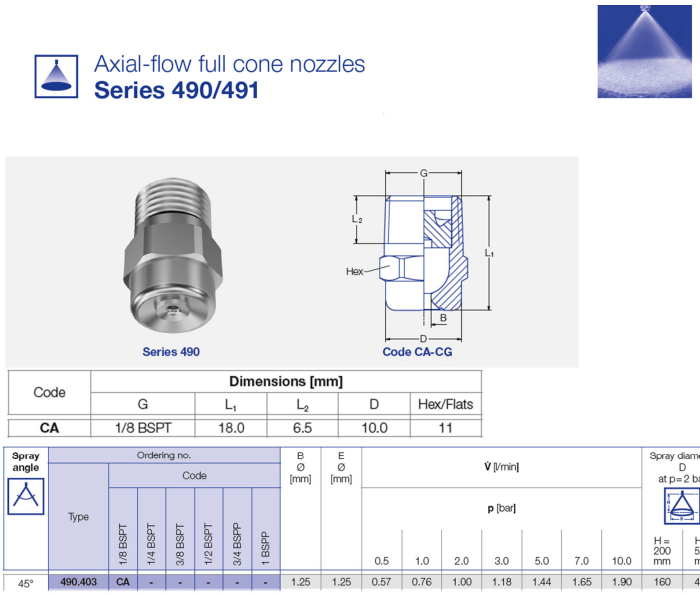

Code	Dimensions [mm]				
	G	L_1	L_2	D	Hex/Flats
CA	1/8 BSPT	18.0	6.5	10.0	11

Spray angle	Ordering no.							B Ø [mm]	E Ø [mm]	V̇ [l/min]							Spray diameter D at p=2 bar	
	Type	Code								p [bar]								
		1/8 BSPT	1/4 BSPT	3/8 BSPT	1/2 BSPT	3/4 BSPP	1 BSPP			0.5	1.0	2.0	3.0	5.0	7.0	10.0	H = 200 mm	H = 500 mm
45°	490.403	CA	-	-	-	-	-	1.25	1.25	0.57	0.76	1.00	1.18	1.44	1.65	1.90	160	400

Figure A1. Nozzle description.

Appendix B

Table A1. Experimental data.

State No.	Packed Bed	V_a Nm^3/h	ϕ_{a1} %	$T_{\phi 1}$ °C	x_{a1} kg/kg	V_w L/min	T_{w1} °C	T_{w2} °C	T_{a1} °C	T_{a2} °C	ϕ_{a2} %	x_{a2} kg/kg
1	RR 1400	2.7	44%	17.3	0.005	0.921	61.7	54.6	17.5	59.9	100%	0.154
2	RR 1400	3.4	44%	17.3	0.005	0.934	61.6	53.4	17.5	59.3	100%	0.149
3	RR 1400	4	44%	17.3	0.005	0.931	61.6	51.8	17.5	58.5	100%	0.142
4	RR 1400	6	44%	17.3	0.005	0.934	62.2	49.9	17.5	57.6	100%	0.135
5	RR 1400	8	44%	17.3	0.005	0.919	62.8	47.7	17.5	56.4	100%	0.126
6	RR 1400	10	44%	17.3	0.005	0.918	63.3	45.8	17.5	55.1	100%	0.117
7	RR 1400	12	44%	17.3	0.005	0.927	63.6	44.3	17.5	54.0	100%	0.110
8	RR 300	2.7	44%	17.3	0.005	0.929	63.0	56.2	17.5	59.5	100%	0.151
9	RR 300	3.4	44%	17.3	0.005	0.947	61.9	54.3	17.5	57.9	100%	0.138
10	RR 300	4	44%	17.3	0.005	0.936	62.0	53.3	17.5	57.5	100%	0.134
11	RR 300	6	44%	17.3	0.005	0.925	62.1	50.5	17.5	55.7	100%	0.121
12	RR 300	8	44%	17.3	0.005	0.927	62.5	48.6	17.5	54.4	100%	0.113
13	RR 300	10	44%	17.3	0.005	0.930	62.8	47.0	17.5	53.2	100%	0.105
14	RR 300	12	44%	17.3	0.005	0.925	63.3	45.6	17.5	52.1	100%	0.099
15	-	2.7	44%	17.3	0.005	0.924	60.5	54.5	17.4	56.1	100%	0.124
16	-	3.4	44%	17.3	0.005	0.936	60.9	53.9	17.4	55.7	100%	0.121
17	-	4	44%	17.3	0.005	0.921	61.1	53.0	17.4	55.2	100%	0.117
18	-	6	44%	17.3	0.005	0.928	60.9	51.1	17.4	53.8	100%	0.108
19	-	8	44%	17.3	0.005	0.918	63.0	50.4	17.4	53.8	100%	0.109
20	-	10	44%	17.3	0.005	0.926	62.7	48.2	17.4	52.0	100%	0.098
21	-	12	44%	17.3	0.005	0.922	61.7	46.4	17.4	50.0	100%	0.088
22	RR 1400	2.7	31%	13.6	0.003	0.940	42.0	39.4	13.9	41.7	100%	0.055
23	RR 1400	4	31%	13.6	0.003	0.940	42.3	38.5	13.9	41.6	100%	0.054
24	RR 1400	6	31%	13.6	0.003	0.940	43.2	37.9	13.9	41.7	100%	0.055
25	RR 1400	8	31%	13.6	0.003	0.933	44.0	37.1	13.9	41.5	100%	0.054
26	RR 1400	10	31%	13.6	0.003	0.924	44.7	36.3	13.9	41.3	100%	0.053
27	RR 1400	12	31%	13.6	0.003	0.948	45.3	35.6	13.9	40.8	100%	0.052

Table A1. *Cont.*

State No.	Packed Bed	V_a Nm^3/h	ϕ_{a1} %	$T_{\phi 1}$ °C	x_{a1} kg/kg	V_w L/min	T_{w1} °C	T_{w2} °C	T_{a1} °C	T_{a2} °C	ϕ_{a2} %	x_{a2} kg/kg
28	RR 300	2.7	31%	13.6	0.003	0.933	42.7	40.2	13.7	41.6	100%	0.054
29	RR 300	4	31%	13.6	0.003	0.921	42.9	39.0	13.7	41.0	100%	0.053
30	RR 300	6	31%	13.6	0.003	0.932	43.3	38.0	13.7	40.6	100%	0.051
31	RR 300	8	31%	13.6	0.003	0.923	43.5	37.2	13.7	39.9	100%	0.049
32	RR 300	10	31%	13.6	0.003	0.930	43.6	36.0	13.7	39.1	100%	0.047
33	RR 300	12	31%	13.6	0.003	0.954	43.7	35.3	13.7	38.5	100%	0.045
34	-	2.7	31%	13.6	0.003	0.936	43.0	40.5	13.7	41.1	100%	0.053
35	-	4	31%	13.6	0.003	0.932	43.0	39.4	13.7	40.2	100%	0.050
36	-	6	31%	13.6	0.003	0.926	43.0	38.2	13.7	39.3	100%	0.048
37	-	8	31%	13.6	0.003	0.939	43.1	37.3	13.7	38.5	100%	0.046
38	-	10	31%	13.6	0.003	0.931	43.1	36.3	13.7	37.7	100%	0.043
39	-	12	31%	13.6	0.003	0.922	42.9	35.2	13.7	36.7	100%	0.041

Appendix C

Table A2. Energy and mass balances.

State No.	$Q_{in} = Q_w$ kW	Q_a kW	Q_{loss} kW	Q_{out} [1] kW	diffr. [2] %	m_{w1} kg/h	m_{da} kg/h	m_{wv1} kg/h	m_{w2} kg/h	m_{wv2} kg/h
1	0.48	0.42	0.02	0.44	9.7	54.4	3.46	0.02	53.9	0.53
2	0.57	0.50	0.02	0.52	7.5	55.1	4.36	0.02	54.5	0.65
3	0.67	0.57	0.02	0.59	12.8	55.0	5.13	0.03	54.3	0.73
4	0.85	0.81	0.02	0.83	3.0	55.2	7.70	0.04	54.2	1.04
5	1.03	1.01	0.02	1.03	−0.3	54.3	10.3	0.06	53.1	1.30
6	1.18	1.17	0.02	1.19	−0.6	54.3	12.8	0.07	52.9	1.51
7	1.32	1.32	0.02	1.34	−1.6	54.9	15.4	0.08	53.3	1.69
8	0.47	0.41	0.02	0.43	9.5	54.8	3.46	0.02	54.3	0.52
9	0.53	0.47	0.02	0.49	8.9	55.9	4.36	0.02	55.3	0.60
10	0.61	0.54	0.02	0.56	8.3	55.3	5.13	0.03	54.6	0.69
11	0.79	0.73	0.02	0.74	6.0	54.7	7.70	0.04	53.8	0.93
12	0.95	0.90	0.02	0.92	3.1	54.8	10.3	0.06	53.7	1.16
13	1.09	1.05	0.02	1.07	1.7	55.0	12.8	0.07	53.7	1.35
14	1.20	1.18	0.02	1.20	0.2	54.7	15.4	0.08	53.3	1.52
15	0.41	0.33	0.02	0.35	14.1	54.6	3.46	0.02	54.2	0.43
16	0.48	0.41	0.02	0.43	11.0	55.3	4.36	0.02	54.8	0.53
17	0.55	0.47	0.02	0.49	11.0	54.4	5.13	0.03	53.8	0.60
18	0.68	0.65	0.02	0.67	1.1	54.9	7.70	0.04	54.1	0.83
19	0.86	0.87	0.02	0.89	−2.9	54.3	10.3	0.06	53.2	1.12
20	0.99	0.99	0.02	1.00	−0.8	54.8	12.8	0.07	53.6	1.26
21	1.04	1.05	0.02	1.07	−2.2	54.5	15.4	0.08	53.3	1.35
22	0.18	0.15	0.01	0.17	5.0	56.0	3.47	0.01	55.8	0.19
23	0.26	0.23	0.01	0.24	7.2	56.0	5.14	0.02	55.7	0.28
24	0.36	0.34	0.01	0.36	1.5	56.0	7.72	0.02	55.6	0.42
25	0.47	0.45	0.01	0.47	0.0	55.5	10.3	0.03	55.0	0.56
26	0.57	0.56	0.01	0.57	−1.1	55.0	12.9	0.04	54.4	0.69
27	0.67	0.66	0.01	0.67	−0.8	56.4	15.4	0.05	55.7	0.80
28	0.17	0.15	0.01	0.17	−0.1	55.5	3.47	0.01	55.3	0.19
29	0.26	0.22	0.01	0.23	10.6	54.8	5.14	0.02	54.6	0.27
30	0.35	0.32	0.01	0.34	4.8	55.5	7.72	0.02	55.1	0.40
31	0.42	0.42	0.01	0.43	−0.9	54.9	10.3	0.03	54.5	0.51
32	0.51	0.50	0.01	0.51	−0.3	55.4	12.9	0.04	54.8	0.61
33	0.58	0.57	0.01	0.59	−1.0	56.8	15.4	0.05	56.2	0.70
34	0.17	0.15	0.01	0.16	3.1	55.7	3.47	0.01	55.5	0.18
35	0.24	0.21	0.01	0.22	7.0	55.4	5.14	0.02	55.2	0.26
36	0.32	0.30	0.01	0.31	1.4	55.1	7.72	0.02	54.8	0.37
37	0.40	0.38	0.01	0.39	0.8	55.9	10.3	0.03	55.4	0.47
38	0.46	0.46	0.01	0.47	−1.2	55.4	12.9	0.04	54.9	0.56
39	0.51	0.52	0.01	0.53	−2.3	54.9	15.4	0.05	54.3	0.63

[1] $Q_{out}=Q_a+Q_{loos}$; [2] diffrence.

References

1. Scheuch, Maxixum Energy Gain from Flue Gas. Available online: https://www.scheuch.sk/wp-content/uploads/2023/03/Scheuch_Folder_ERCS_E_Web.pdf (accessed on 27 March 2025).
2. LAB, Combustion Air Humidification. Available online: https://www.lab.fr/en/combustion-air-humidification-0# (accessed on 27 March 2025).
3. Dlouhý, T.; Havlík, J. Effect of combustion air humidification on the operation of a biomass boiler—Theoretical analysis. *Heliyon* **2025**, *11*, e42299. [CrossRef] [PubMed]
4. Hewitt, G.F.; Shires, G.L.; Bott, T.R. *Process Heat Transfer*; Begell House: New York, NY, USA, 1994. [CrossRef]
5. Zhang, Y.; Du, C.; Zhang, Z.; Du, J.; Tu, Y.; Ren, Z. Process Intensification of Gas–Liquid Separations Using Packed Beds: A Review. *Separations* **2024**, *11*, 284. [CrossRef]
6. Garg, K.; Das, S.K.; Tyagi, H. Thermal design of a humidification-dehumidification desalination cycle consisting of packed-bed humidifier and finned-tube dehumidifier. *Int. J. Heat Mass Transf.* **2022**, *183*, 122153. [CrossRef]
7. VDI-GVC. (Ed.) *VDI Heat Atlas*; Springer: Berlin/Heidelberg, Germany, 2010. [CrossRef]
8. Morales, A.A.; Carvajal, D.S. Heat and mass transfer in a direct contact humidifier of a humidification-dehumidification desalination system. In Proceedings of the 2017 IEEE 6th International Conference on Renewable Energy Research and Applications (ICRERA), San Diego, CA, USA, 5–8 November 2017; pp. 273–278. [CrossRef]
9. Chen, Q.; Thu, K.; Bui, T.D.; Li, Y.; Ng, K.C.; Chua, K.J. Development of a model for spray evaporation based on droplet analysis. *Desalination* **2016**, *399*, 69–77. [CrossRef]
10. Hijjaji, K.; Gabsi, S.; Frikha, N. Determination of heat and mass transfer coefficients in a spray humidifier of a humidification–dehumidification desalination system. *Desalination Water Treat.* **2021**, *225*, 392–401. [CrossRef]
11. Toman, F.; Kracík, P.; Pospíšil, J. Heat transfer during condensation of water vapour in the presence of non-condensable gas in vertical tube of small diameter. *Case Stud. Therm. Eng.* **2022**, *40*, 102519. [CrossRef]
12. Garg, K.; Beniwal, R.; Das, S.K.; Tyagi, H. Experimental investigation of a low-cost humidification-dehumidification desalination cycle using packed-bed humidifier and finned-tube heat exchanger. *Therm. Sci. Eng. Prog.* **2023**, *41*, 101858. [CrossRef]
13. Flagiello, D.; Parisi, A.; Lancia, A.; Di Natale, F. A Review on Gas-Liquid Mass Transfer Coefficients in Packed-Bed Columns. *ChemEngineering* **2021**, *5*, 43. [CrossRef]
14. Zhu, Q.; Wu, W.; Ren, Y.; Wang, F.; Han, Y. Study on the Heat and Mass Transfer Characteristics of Humidifiers in Humidification–Dehumidification Desalination Systems. *Energies* **2023**, *16*, 8006. [CrossRef]
15. Huang, X.; Chen, H.; Ling, X.; Liu, L.; Huhe, T. Investigation of heat and mass transfer and gas–liquid thermodynamic process paths in a humidifier. *Energy* **2022**, *261*, 125156. [CrossRef]
16. Chen, J.; Han, D.; He, W.; Liu, Y.; Gu, J. Theoretical and experimental analysis of the thermodynamic and economic performance for a packed bed humidifier. *Energy Convers. Manag.* **2020**, *206*, 112497. [CrossRef]
17. Onda, K.; Takeuchi, H.; Okumoto, Y. Mass transfer coefficients between gas and liquid phases in packed columns. *J. Chem. Eng. Jpn.* **1968**, *1*, 56–62. [CrossRef]
18. Klimanek, A. Numerical Modelling of Natural Draft Wet-Cooling Towers. *Arch. Comput. Methods Eng.* **2016**, *20*, 61–109. [CrossRef]
19. Sezen, K.; Gungor, A. Water droplet evaporation in atmospheric air stream. *Phys. Fluids* **2023**, *35*, 017122. [CrossRef]
20. Chen, J.; Han, D.; He, W.; Ji, C.; Si, Z.; Zheng, M.; Gu, J.; Song, Y. Characteristic analysis of heat and mass transfer process within structured packing humidifier. *J. Braz. Soc. Mech. Sci. Eng.* **2019**, *41*, 361. [CrossRef]
21. Joint Committee for Guides in Metrology (JCGM). *Evaluation of Measurement Data—Guide to the Expression of Uncertainty in Measurement*; Bureau International des Poids et Mesures: Sèvres, France, 2008. Available online: https://www.bipm.org/documents/20126/2071204/JCGM_100_2008_E.pdf/cb0ef43f-baa5-11cf-3f85-4dcd86f77bd6 (accessed on 27 March 2025).
22. Farrance, I.; Frenkel, R. Uncertainty of measurement: A review of the rules for calculating Uncertainty components through functional relationships. *Clin. Biochem. Rev.* **2012**, *33*, 49–75. [PubMed]

Disclaimer/Publisher's Note: The statements, opinions and data contained in all publications are solely those of the individual author(s) and contributor(s) and not of MDPI and/or the editor(s). MDPI and/or the editor(s) disclaim responsibility for any injury to people or property resulting from any ideas, methods, instructions or products referred to in the content.